

CHARACTERIZATION OF THE RADIATION ENVIRONMENT AT THE ARMY PULSE RADIATION FACILITY WITH MONTE CARLO

JOHN C. WAGNER and ANTHONY J. BARATTA
Nuclear Engineering Department, Penn State University
231 Sackett Building, University Park, PA 16802, USA
E-mail: wagner@gracie.psu.edu, ab2@psuvm.psu.edu

and

JOHN W. GERDES
U.S. Army Pulse Radiation Facility
Aberdeen Proving Ground, MD 21005, USA
E-mail: jgerdes@apg-9.apg.army.mil

ABSTRACT

Coupled neutron-gamma Monte Carlo calculations are performed to characterize the radiation environment at the Army Pulse Radiation Facility Reactor (APRFR). The APRFR is a bare, fast reactor that is used for testing the survivability of sensitive electronic and optical devices in radiation environments that are often difficult, or even impossible, to measure. Therefore, it is essential that the radiation environment surrounding the APRFR be accurately determined through transport calculations. Responding to this exigency, a detailed three-dimensional model of the APRFR has been developed for the Monte Carlo code MCNP. Calculated results are compared to measured data and preexisting calculated results from an independent organization. For analysis purposes, the effects of using continuous energy ENDF/B-V and ENDF/B-VI and multigroup (DABL69) cross sections are briefly discussed.

1. Introduction

The Army Pulse Radiation Facility Reactor (APRFR) is a bare fast, highly-enriched uranium-molybdenum cylindrical reactor that is enclosed in an aluminum silo 30 meters in diameter and 20 meters in height. The reactor is suspended from a transporter device that allows it to be moved to a number of experimental locations. The main purpose of the APRFR is to simulate pulse radiation environments for testing the survivability of sensitive electronic and optical devices. Direct measurement of these radiation environments in detail is impossible in most instances, yet it is essential that a reasonably accurate estimate be made so that the test results obtained at the APRFR can be appropriately related to survivability. This requires characterization of the radiation environments for the various testing configurations through transport calculations.

In the past, numerous attempts, with varying degrees of success, have been made to characterize the APRFR radiation environment with the discrete ordinates DORT

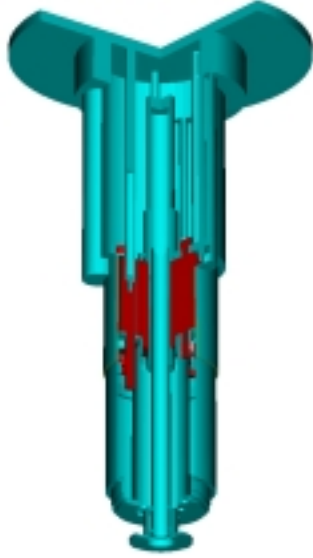


Fig. 1 APRFR Model

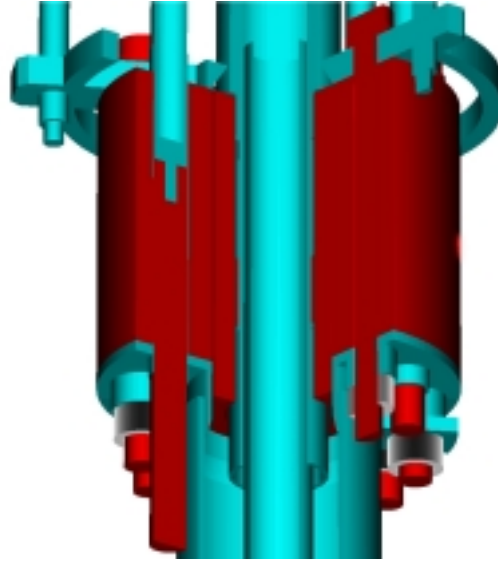


Fig. 2. APRFR Core

code¹. However, inconsistencies between calculations and measurements of various important aspects of the APRFR radiation environment have persisted. It is believed that these inconsistencies can be attributed to geometric approximations associated with modeling an intricate three-dimensional reactor in two dimensions and the data approximations associated with multigroup cross sections. Therefore, it is necessary to model the APRFR with a more accurate method. The Monte Carlo method offers explicit three-dimensional geometric representation and continuous energy simulation, and thus, is well suited for this task. In this work we apply the radiation transport code MCNP (version 4A)² to the calculation of the APRFR radiation environment.

2. MCNP Modeling

A detailed three-dimensional model of the APRFR has been developed for MCNP. This model extends axially from the bottom of the borated concrete floor to the top of the 1 inch thick steel support plate, and radially out to 10 meters. The reactor transporter and surrounding structures are approximated.

The degree of detail is indicated in Figs. 1 and 2, which show three-dimensional views of the MCNP model as prepared by the SABRINA code³. The different shades of gray in the figures represent different materials; the darkest of which is the fuel. All components in the direct vicinity of the core region are modeled exactly, with the exception of the hexagonal bolt heads modeled as cylinders and bolt threads approximated. In modeling the fuel (i.e., cylindrical plates, fuel bolts, and safety block), the actual dimensions and masses as physically measured by the APRFR staff were used to describe the components and determine densities such that the mass of each component was conserved.

To facilitate the comparison of calculated parameters to previously calculated results and to measured quantities, two slightly different models were created. The first model describes the free-in-air reactor configuration and is used for comparison to previously calculated results and measured doses. The second model represents the reactor next to the Electronics Exposure Table (EET) to calculate activities for comparison with measured values. These two models are identical with the following exceptions: (1) the regulating rod height and (2) the presence of the EET.

Unless otherwise stated, the “recommended” continuous energy cross sections² (mostly based on ENDF/B-V) were used for the transport calculations and the SNL-RML Dosimetry cross sections⁴ were used in the activity calculations. For analysis purposes, the continuous energy ENDF/B-VI cross sections and the DABL69 multigroup cross-section library⁵ were also used. The DABL69 multigroup library is relevant for comparison to the results of previous investigators.

3. Discussion of Results

3.1. Criticality calculations

All k_{eff} values reported herein are based on the covariance-weighted combination of the collision, absorption, and track length k_{eff} estimators. The covariance-weighted combination is quoted because it incorporates all the k_{eff} estimates generated by MCNP. In all cases, the initial guess for k_{eff} was 1.0, and the results are based on 200 total cycles with ~ 12000 neutrons/cycle. The calculated values of k_{eff} and the corresponding estimated 1σ uncertainties are given in Table 1. All k_{eff} values calculated with continuous energy cross sections are slightly lower than unity (within $\sim 0.35\%$). These results were expected, as it is not practical to model the entire reactor bay area, and therefore neutrons that are being returned to the core from various structures inside the reactor bay are not being accounted for. These results demonstrate that the effect is $< 0.5\%$.

The effect of the ENDF/B-VI cross sections is small for this eigenvalue calculation. This result was expected since similar findings have been previously reported⁶. The k_{eff} values calculated with the DABL69 multigroup cross sections are both slightly higher ($\sim 0.6\%$) than unity. Considering the fact that the DABL69 library is intended for defense-related shielding problems, this result is quite good.

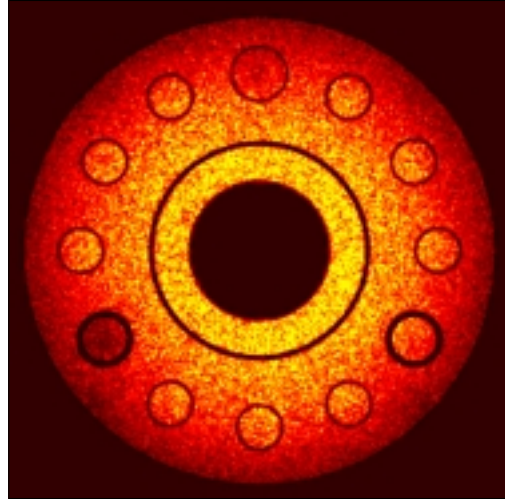
The spatial fission density (integrated over the axial direction) is plotted in Fig. 3. The fission density figure is based on 800,000 fission positions, which are taken from the MCNP *srctp* file. The lighter regions represent higher fission density and the black regions correspond to the absence of fission events. Thus, the figure clearly shows the non-fissile regions and the appropriate behavior within the core.

3.2. Comparison to Previously Calculated Results

Previous to this work, analysts at Science Applications International Corporation (SAIC) modeled the APRFR and characterized its’ radiation environment⁷ with the

Table 1. k_{eff} Values for the APRFR Models

Data	Free-In-Air Model	EET Model
B-V	0.9984(4.2-4) ^{a,b}	0.9980(4.2-4)
B-VI	0.9974(4.3-4)	0.9965(4.6-4)
DABL	1.0062(5.0-4)	1.0055(5.7-4)

^a 1σ uncertainties^b read as 4.2E-04**Fig. 3.** Fission Density in the APRFR

discrete ordinates DORT code using the DABL69 multigroup library. This work was based on a two-dimensional r-z model.

Figure 4 shows the ratios of the SAIC results to our results with MCNP, labeled *PSU (MCNP)*, for the 2 meter neutron leakage spectrum. The error bars in this figure and all subsequent figures correspond to 1σ statistical uncertainties. The agreement appears to be reasonable. However, our results are 10-30% higher in the intermediate energy range (0.005-1.0 MeV). Because the SAIC results were reported to be low in this energy range with respect to measurements⁸, these results are desirable and represent a significant improvement.

Figure 5 shows the ratios of the SAIC results to our results for the 2 meter gamma leakage spectrum (without the contribution from delayed gammas), and reveals reasonable agreement over a major portion of the energy range. However, there is a clear divergence of agreement for energies below ~ 0.5 MeV. Further analysis of these differences, in the form of multigroup MCNP calculations with the DABL69 library, demonstrated that most of the discrepancies can be attributed to the DABL69 cross-section library.

3.3. Comparison to Measured Results

In this section, MCNP results are compared to measured data. These measured data include: foil activities and a subsequently derived neutron spectrum at 29 cm from the core centerline and neutron and gamma doses at 1, 2, and 5 meters⁹.

The free-field foil data¹⁰ were taken on the EET, with the reactor midplane approximately 66 inches above the borated concrete floor. The spectrum based on measurements was unfolded by the SAND-II code¹¹ which, with an initial trial spectrum, iterates to determine the spectrum. Unfortunately, the shape of the spectrum generated by SAND-II was found to be sensitive to the initial trial spectrum and to the exclusion of even a single foil activity. Therefore, there is an uncertainty associated with the unfolded spectrum that is not easily quantified. Figure 6 compares

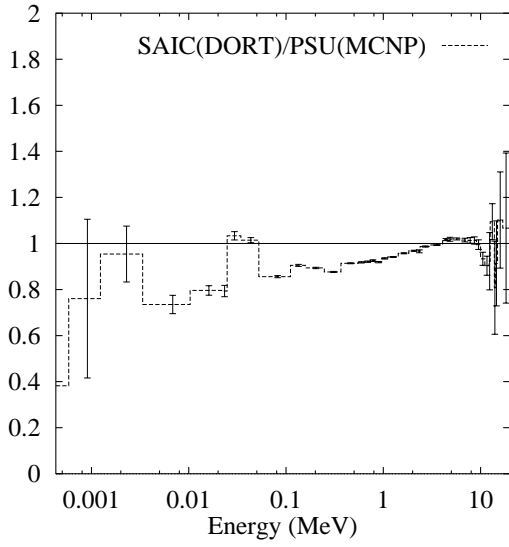


Fig. 4. Neutron Leakage at 2 meters

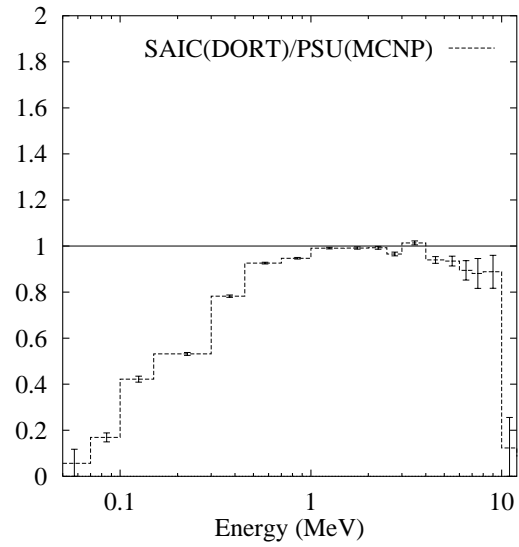


Fig. 5. Gamma Leakage at 2 meters

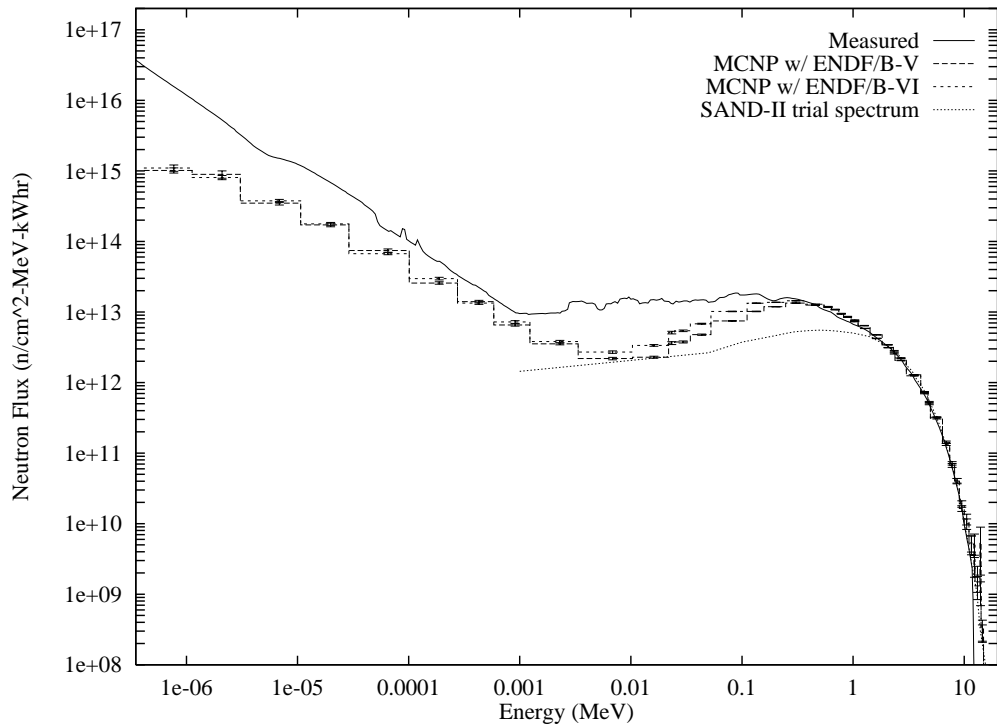


Fig. 6. Comparison of Free-Field Neutron Spectra at 29 cm

Table 2. Free-Field Foil Activities at 29 cm

Reaction	Energy ^a Range (MeV)	Measured ($\frac{dis/s}{nucleus}$)	Calculated ^b ($\frac{dis/s}{nucleus}$)	Ratio ($\frac{calc}{meas}$)
⁹⁰ Zr(n,2n) ⁸⁹ Zr	1.28E+1 - 1.69E+1	3.569E-21	3.668E-21 (.097)	1.028
²⁴ Mg(n,p) ²⁴ Na	6.50E+0 - 1.17E+1	2.127E-19	2.814E-19 (.012)	1.323
²⁷ Al(n,a) ²⁴ Na	6.50E+0 - 1.21E+1	1.048E-19	1.328E-19 (.014)	1.268
⁴⁸ Ti(n,p) ⁴⁸ Sc	5.90E+0 - 1.24E+1	1.347E-20	1.716E-20 (.013)	1.274
³² S(n,p) ³² P	2.40E+0 - 7.50E+0	4.709E-19	4.761E-19 (.002)	1.011
⁵⁸ Ni(n,p) ⁵⁸ Co	2.00E+0 - 7.60E+0	1.472E-19	1.592E-19 (.002)	1.082
⁴⁷ Ti(n,p) ⁴⁷ Sc	1.90E+0 - 7.60E+0	6.700E-19	5.798E-19 (.002)	0.865
¹¹⁵ In(n,n') ^{115m} In	1.00E+0 - 6.00E+0	1.078E-16	1.162E-16 (.004)	1.078
¹⁰³ Rh(n,n') ¹⁰³ Rh	5.50E-1 - 5.70E+0	2.171E-15	2.949E-15 (.001)	1.358
⁴⁵ Sc(n,γ) ⁴⁶ Sc	4.25E-7 - 1.00E+0	1.180E-19	2.610E-20 (.002)	0.221
¹⁹⁷ Au(n,γ) ¹⁹⁸ Au	4.00E-6 - 7.20E-4	6.357E-17	1.771E-17 (.034)	0.279
¹⁹⁷ Au(n,γ) ¹⁹⁸ Au (Cd covered)	4.00E-6 - 7.20E-4	5.010E-17	1.531E-17 (.029)	0.306

^a Energy limits inside of which 95% of the detector response occurs for each reaction (for a fast burst spectrum)¹²

^b Numbers in parenthesis are 1σ uncertainties

the unfolded and calculated neutron spectra at 29 cm from the core centerline. The agreement is shown to be good above ~0.2 MeV, and quite poor for intermediate and thermal energies. Also, the ENDF/B-VI cross sections are shown to improve the agreement in the range 0.003-0.02 MeV.

In an effort to better understand the differences, MCNP (with ENDF/B-VI) was used to calculate several of the foil activities directly. These calculated activities are compared to the measured activities in Table 2. In general, the calculated activities for reactions that are more sensitive to high energy neutrons are higher (within ~30%) than the measured activities. On the other hand, the calculated activities for reactions that are more sensitive to low energy neutrons (e.g., ⁴⁵Sc(n,γ)⁴⁶Sc and ¹⁹⁷Au(n,γ)¹⁹⁸Au) are significantly lower than the measured activities.

In an attempt to understand these differences, the origin of the neutrons contributing to the 29 cm spectrum was investigated. Figure 7 shows the total spectrum and its two components; (1) the neutrons coming directly from the core and (2) the neutrons arriving at the 29 cm location after interacting with the ex-core regions. From this figure, it seems that the ex-core regions are solely responsible for producing neutrons in the thermal range and that they also contribute significantly to the intermediate (0.01-1.0 MeV) range. However, more accurate modeling of the reactor surroundings has not resolved these discrepancies.

For the measurement of neutron and gamma doses, the reactor was situated 5 meters above the floor, with the detectors at the same height, to minimize the effects

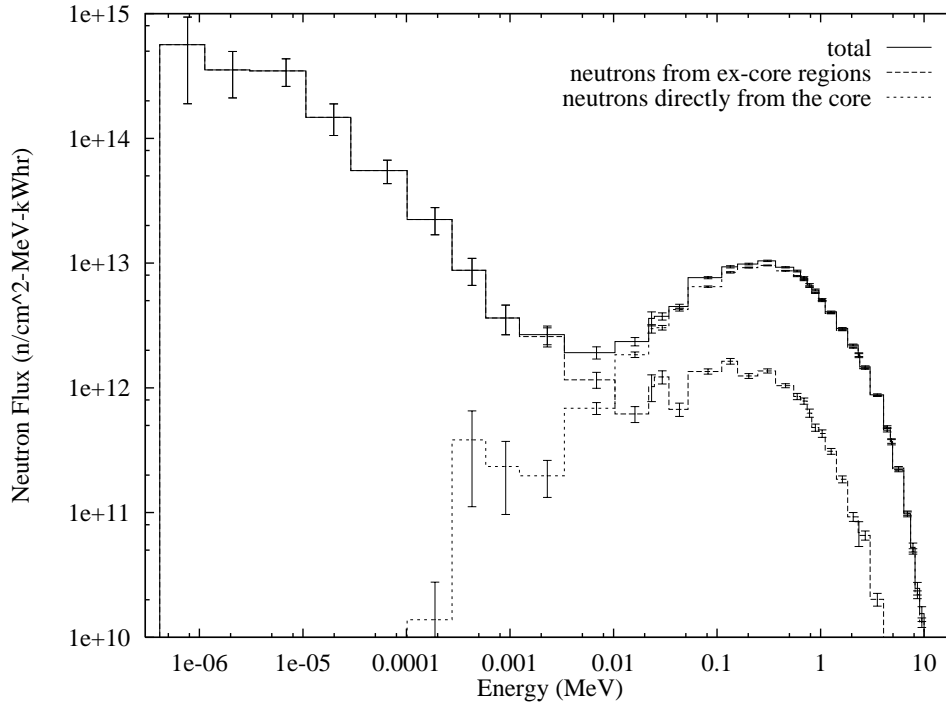


Fig. 7. Examination of Neutron Spectra at 29 cm

of radiation interacting with the floor⁹. Therefore, the MCNP free-in-air model was used to generate the results for this comparison.

Measured and independently calculated neutron and gamma doses are compared in Table 3. The agreement between all three of the neutron doses is quite good. In fact, the difference between the PSU calculated results and the measured neutron doses are within $\sim 5\%$. For the gamma doses, good agreement (within 15%) with the measured results is achieved. However, before including the effect of delayed fission gammas, our results were similar to those calculated by SAIC. Because the APRFR is a bare fast reactor, the delayed gammas are not attenuated, and thus represent a significant portion of the total gamma dose.

Table 3. Free-Fielded Tissue Doses (Rad/kWhr)

Distance (m)	Measured		SAIC Calculated ⁹		PSU Calculated ^a	
	Neutron	Gamma	Neutron	Gamma	Neutron	Gamma
1	2905.0	305.0	2700.0	175.0	2859.9(.001)	269.1(.007)
2	700.0	65.0	737.0	44.5	713.8(.001)	66.2(.004)
5	137.6	12.3	132.0	7.4	129.4(.001)	10.5(.005)

^a Numbers in parenthesis are 1σ uncertainties

4. Summary

Efforts to characterize the radiation environment at the APRFR by comparing Monte Carlo calculations to measured data and previously calculated results have been discussed. A detailed three-dimensional model of the APRFR for the MCNP code was presented. The calculated results were compared to previously calculated neutron and gamma leakage spectra from an independent organization. Agreement between calculated and measured activities was shown to be good for the reactions that are sensitive to mid-to-high energies and poor for lower energies. More accurate modeling of the reactor surroundings has not resolved these differences. Neutron dose measurements and calculations agree to within $\sim 5\%$. With the inclusion of delayed gammas, the calculated gamma doses are within 15% of the measured doses. Omission of the delayed gammas, results in a significant underestimation (as much as 50%) of the gamma dose.

5. References

1. W.A. RHOADES and R.L. CHILDS, "The DORT Two-Dimensional Discrete Ordinates Transport Code System," CCC-484, ORNL-RSICC, Oak Ridge, TN (1989).
2. J.F. BRIESMEISTER, Editor, "MCNP – A General Monte Carlo N-Particle Transport Code, Version 4A," Los Alamos National Laboratory report LA-12625, (1993).
3. K.A. VAN RIPER, "SABRINA: Three-Dimensional Geometry Visualization Code System," PSR-242, ORNL-RSICC, Oak Ridge, TN (1993).
4. P.J. GRIFFIN, J.G. KELLY, T.F. LUERA, and J. VANDENBURG, "SNLRML Recommended Dosimetry Cross Section Compendium," DLC-178, ORNL-RSICC, Oak Ridge, TN (1993).
5. "DABL69: Defense Nuclear Applications Broad-Group Library Based on ENDF/B-V in ANISN format," DLC-130, ORNL-RSICC, Oak Ridge, TN (1989).
6. D.C. KAUL and S.D. EGBERT, "Radiation Leakage from the Army Pulse Radiation Facility (APRF) Fast Reactor," SAIC-89/1423 (1989).
7. J.S. HENDRICKS, S.C. FRANKLE, and J.D. COURT, "ENDF/B-VI Data for MCNP," Los Alamos National Laboratory report, LA-12891 (1994).
8. D.C. KAUL and S.D. EGBERT, "Radiation Fluences at the Army Pulse Radiation Facility (APRF) Fast Reactor," SAIC-90/1286 (1990).
9. C.R. HEIMBACH, "Final Report of the Gamma-Ray Leakage from the Aberdeen Pulse Radiation Facility (APRF) Reactor," Report No. CSTA-7696 (April 1995).
10. M.A. OLIVER, "Research Report of the Pin Diode and Neutron Spectrum Measurements at the Army Pulse Radiation Facility," Report No. ATC-7847 (1996).
11. "SNL SAND-II: Neutron Flux Spectra Determination by Multiple Foil Activation - Iterative Method", PSR-345, ORNL-RSICC, Oak Ridge, TN (1994).
12. ASTM Standard E720-94, "Standard Guide for Selection and Use of Neutron-Activation Foils for Determining Neutron Spectra Employed in Radiation-Hardness Testing of Electronics," 1995 Annual Book of ASTM Standards, Vol. 12.02 (1995).